

Diamond-like film as a corrosion protective layer on the hard disk

B. Tomcik^{a,*}, T. Osipowicz^b, J.Y. Lee^c

^aData Storage Institute, DSI Building, 5, Engineering Drive 1, Singapore 117608, Singapore

^bDepartment of Physics, National University of Singapore, Singapore 0511, Singapore

^cDepartment of Chemical Engineering, National University of Singapore, Singapore 119260, Singapore

Received 1 September 1998; received in revised form 12 October 1999; accepted 12 November 1999

Abstract

A magnetic layer based on Co-alloys does not possess the necessary mechanical durability and corrosion resistance and must be covered with a protective layer. An accelerated electrochemical test has been conducted on a hard disk magnetic layer covered with amorphous hydrogenated carbon doped with nitrogen. From the potentiodynamic and DC polarization measurements of the corrosion current in a 0.15 M NaCl solution adjusted to different pH, it was concluded that an acid environment can largely decrease the reliability and lifetime of a hard disk. Lubricant can contribute to corrosion protection by covering voids and other overcoat imperfections and prevent water vapor penetration into the magnetic film. Atomic force microscope images show localized distribution of corrosion sites with a density of 1.2×10^6 defects/cm². The overcoat also prevents a lateral spread of the corrosion products across a disk. © 2000 Elsevier Science S.A. All rights reserved.

Keywords: Carbon; Corrosion; Surface defects

1. Introduction

Diamond-like carbon (DLC) film has been extensively used in the hard disk drive industry as a wear and corrosion protective overcoat on the magnetic layer. Currently, various types of amorphous carbon a-C, hydrogenated amorphous carbon with or without nitrogen a-C:H(N), as a single layer or in combination, are in use [1,2]. Doping of amorphous carbon and a-C:H films by nitrogen and properties of C–N structures have been the subject of many theoretical and experimental works [3–8]. Incorporation of nitrogen usually leads to the reduction of the film internal stress and the improvement of the macroscopic corrosion resistance. At the same time this type of structure is accompanied by increased density of voids and higher surface roughness that may have microscopic detrimental effect.

Corrosion is usually initiated at the overcoat imperfection sites, on pinholes, places of large compositional inhomogeneity in the magnetic layer or on the sites with induced stresses. The film stress develops during a film growth and is induced by the substrate texture. Overcoat properties that directly influence the corrosion behavior of the magnetic

layer are porosity, surface roughness and electrical conductivity. Voids in the carbon amorphous structure as well as pinholes in the matrix, being formed through the island film growing mechanism, are permeable to water, environmental oxygen and metal ions. The thickness of the sputter deposited carbon overcoat used by the hard disk industry is around 8 nm. There is a trend of thickness reduction to 3–5 nm till the end of this decade. This implies the development of DLC protective films with a small density of imperfections using other techniques, e.g. ion beam deposition, filtered cathodic arc or mass and energy selected ion beams.

As a magnetic layer the quaternary structure of Co alloy that contains more than 75 at.% of Co is commonly used. Additional elements like Cr, Ta and Pt are added to improve the magnetic properties of the layer, i.e. to increase areal recording density, signal to noise ratio and to minimize magnetostriction. Pure Co film dissolves easily in water. It does not create any passivation layer that could minimize or stop its further degradation when exposed to environmental conditions. Corrosion studies have been performed on various binary and ternary Co-based alloys: Co–P [9–11]; Co–Pt and Co–Ni–Pt [12], using the simple test of film immersion in water and subsequent observation of macroscopic magnetic properties; Co–Ni [10,11]; various cobalt-based alloys with different undercoats and substrates [13]; Co–Cr with and without overcoat [10,11,14,15]; and

* Corresponding author. Tel.: +65-874-8624; fax: +65-777-6619.

E-mail address: tomcik@dsi.nus.edu.sg (B. Tomcik)

FeSmN [16]. When deposited as an underlayer to magnetic film, Cr serves to increase the film magneto-crystalline anisotropy. Also, it acts as a barrier layer. Its role is to prevent corrosion dissolution of Ni from the NiP layer of a hard disk, being exposed to an acid environment. In this work the corrosion properties of ternary Co-alloy ($\text{Co}_{81}\text{Cr}_{15}\text{Ta}_4$) were examined with the magnetic layer being protected with nitrogenated sputter deposited a-C:H film and tetrahedral amorphous carbon, ta-C, with a film thickness typically encountered in hard disk media. Carbon protective properties are addressed also with respect to a different pH value of 0.15 M of NaCl solution in contact with the magnetic layer.

In the a-C:H film structure voids of dimension of more than 0.5 nm have been reported [14], through which water molecules of dimension 0.32 nm can easily permeate. Beside water vapor some other gases and vapors are also detrimental to the magnetic layer. The most well known are SO_2 and Cl_2 gas. Also the residual process chemicals and outgasings from the hard disk drive construction components (uncured adhesive components, gaskets, bearings, greases, plasticizers from the plastic parts, metal alloy and case outgassing) can contribute to corrosion. Among the most severe attacking gases that can decrease the lifetime of a hard disk are SO_2 and Cl_2 , originating mostly from the environment and rubber crosslinking agents outgassing. Microscopic corrosion sites can produce magnetic defects resulting in noise, signal deviation or even dropouts.

Corrosion effects on the magnetic layer can be measured by different techniques: by following the changes in the macroscopic magnetic properties, such as saturation magnetization (M_s), remanent magnetization (M_r), coercivity (H_c) and squareness (M_r/M_s) [17], by measuring the changes in electrical resistance $\Delta R/R_0$ for a structure deposited on a glass substrate [18] or using the standard electrochemical test methods.

Corrosion products from the magnetic layer elements are mostly cobalt hydroxides and cobalt chlorides [10,11,14,15]. Electrical conductivity of the carbon overcoat additionally promotes the galvanic corrosion mechanism between the overcoat and a magnetic layer since all three assumptions for this type of corrosion can be fulfilled: (a) electrical dissimilarity between the layers, carbon being at the very top place in the galvanic corrosion series that results in a Co potential difference of over 0.5 V; (b) electrical contact between the layers; and (c) exposure to the corrosive environment. This third condition is only fulfilled at the carbon pores through which the water molecules–electrolyte can reach a magnetic layer. Visible corrosion sites on the carbon overcoat are mainly around such pores. Increased surface roughness enables capillary retention of water vapor from a humid environment. The longer water dwelling time makes the site more prone to corrosion development. The overcoat electrical conductivity provides the return path for electrons created by Co oxidation and participates in galvanic corrosion.

2. Experimental

Samples from the hard disk plate have been analyzed using the three-electrode electrochemical (EC) tester, atomic force microscope (AFM), scanning electron microscope (SEM) and optical microscope. The hard disk structure and its composition have been studied with Rutherford backscattering spectroscopy (RBS) and the particle-induced X-ray emission (PIXE) technique. Electrochemical test was performed on EG&G model 273 potentiostat/galvanostat with a saturated calomel electrode (SCE) as the reference electrode.

The experimental set-up is presented in Fig. 1. The working electrode was attached to the sample of a hard disk, the examined surface of which was previously defined by an adhesive masking tape. For the counter electrode a platinum mesh was selected. Two electrodes were separated by a piece of filter paper wetted in electrolyte, a 0.15 M solution of NaCl in deionized water. Reference SCE ($\text{Hg}/\text{Hg}_2\text{Cl}_2$, saturated KCl) electrode was placed as close as possible to the working and counter electrode, being separated from them by a piece of filter paper wetted in the electrolyte.

While running the EC potentiodynamic analysis the initial potential applied to the working electrode was -0.25 V with respect to the established open-circuit potential. The scanning procedure ended at 0.600 V above the open-circuit potential. The scanning voltage rate was selected at 1 mV/s. The corrosion current was measured between the working electrode (hard disk sample) and a counter (auxiliary) electrode-platinum mesh. Prior to the acquisition a sample was exposed and purged in the electrolyte environment for 20 min. It was not possible to obtain a clearly defined minimum of the open-circuit corrosion current at larger scan rates and on contaminated surfaces. In a scanning region close to the open circuit potential the ‘rounded’ outlook of the potentiodynamic curve can be avoided by selecting the lower scan rate, e.g. 0.5 or 0.25 mV/s. A DC polarization resistance and a time development of the corrosion potential were measured on the same potentiostat. For the AFM study of the hard disk topography the Topometrix unit, model TMX 2010, was used in the contact mode.

Combined RBS and PIXE analysis were performed at the Nuclear Microscopy Facility at the National University of Singapore. A 2 MeV $^4\text{He}^+$ ion beam was utilized to

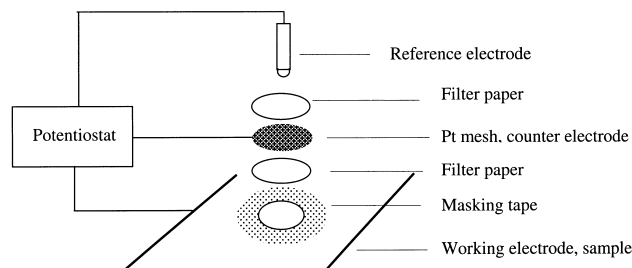


Fig. 1. Experimental set-up for the accelerated electrochemical test.

bombard the surface parallel to the surface normal. The beam on the target had a spot size of approximately 2 mm². Backscattered particles were detected with a silicon charged particle detector positioned at 160° with respect to the outgoing beam. The detector was enclosed in a collimated housing with the solid angle of acceptance of 10 msr and energy resolution of 13 keV. The beam current was measured with a Faraday cup and held between 15 and 25 nA. PIXE measurements were simultaneously carried out with an energy dispersive Si(Li) detector positioned at 45° with respect to the beam. The simultaneous use of PIXE and RBS allowed us to deduce quantitatively the composition of the magnetic film, even in cases where close mass numbers of elements, e.g. of Pt and Ta, severely restricted the RBS analysis.

3. Results and discussion

The carbon overcoat was a DLC film doped with nitrogen and deposited in a DC magnetron sputtering discharge in a gas mixture containing N₂, C₂H₄ and Ar. The lubricated surface was covered with a perfluoropolyether PFPE lubricant. A typical hard disk layered structure investigated by PIXE and RBS measurements is shown in Fig. 2. The points represent the experimental data and the solid line a theoretical spectrum calculated with the RUMP simulation code [19]. The contributions of different elements are indicated separately. The amount of chromium embedded in the Co-alloy can be deduced from a high-energy tail of the Cr peak. The composition and thickness of the carbon overcoat were not precisely analyzed due to the low mass of its constituents and the limited depth resolution of the RBS method. Attempts to detect corrosion-induced and migrated Co on the top of the carbon overcoat failed, even after enhancing

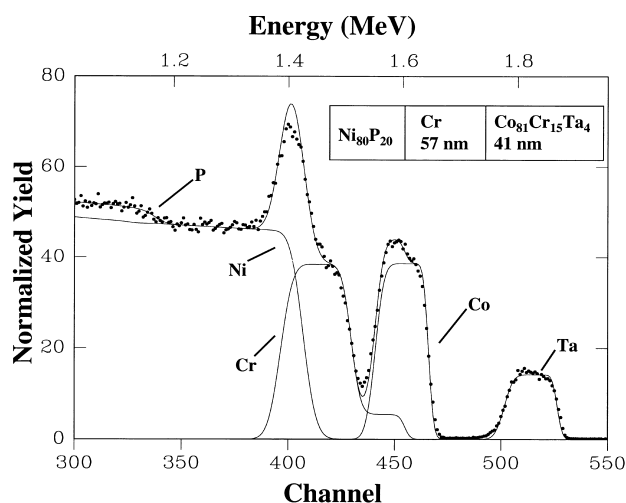


Fig. 2. Composition analysis of the hard disk layer structure with Rutherford backscattering spectroscopy (RBS). The composition of the magnetic layer is found to be Co₈₁Cr₁₅Ta₄.

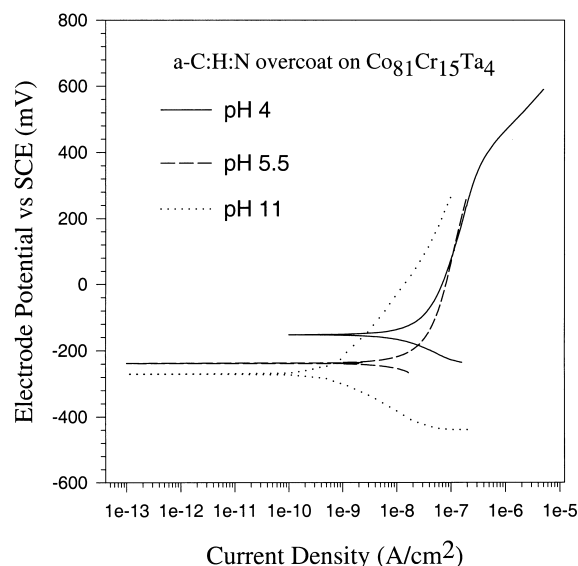


Fig. 3. Potentiodynamic curve of the hard disk overcoat at different pH of 0.15 M NaCl electrolyte.

the RBS surface sensitivity with a graze incidence angle of He⁺ ions.

Electrochemical tests were performed on the non-lubricated hard disk at different pH values of a 0.15 M solution of NaCl. The pH adjustment was achieved by adding droplets of HCl acid and NaOH solution to the base solution. For the determination of corrosion potential and corrosion current a series of potentiodynamic curves was collected on the magnetic layer covered by DLC film, in a similar way as reported in Refs. [11,14].

Each potentiodynamic (E versus $\log i$) curve, as presented in Fig. 3, consists of two branches, the lower one named the cathodic and the upper one the anodic side. The acquisition of the curve started from the potential 0.25 V below the open circuit potential. The anodic part of the curve was run from the open circuit potential to a value of 0.6 V above it. At the open circuit potential the net current flowing in the external circuit is close to zero and is presented as a straight line during the transition from the cathodic to the anodic part of the potentiodynamic curve.

Though the current in the external circuit at the open circuit potential is almost negligible many chemical reactions can take place on the surface. Simultaneously, the anodic and cathodic currents flow on the surface, but in opposite directions. At these 'equilibrium' conditions, an overcoated metal surface acts as an assembly of many tiny anodes and cathodes. The corrosion occurs at a rate given by the theoretical anode current density i_a [20]

$$i_a = \frac{\alpha\beta}{2.3(\alpha + \beta)} \frac{\Delta i}{\Delta E} \quad (1)$$

where α is the anodic and β the cathodic Tafel slope of the potentiodynamic curve expressed in V/current decade, $\Delta i/\Delta E$ is the slope in the linear region of the DC polarization

curve expressed in $\mu\text{A}/\text{V}$ and i_a is the corrosion current in μA .

During the cathodic part of the voltage sweep, the counter electrode-platinum mesh acts as an anode, and therefore will not contaminate the solution with its ions. The required production of electrons on the working electrode (the cathode surface) takes place through the reactions in the aqueous solution. The most important reactions are the generation of oxygen gas from water



and the generation of chlorine gas in the NaCl solution



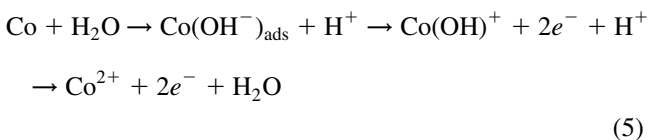
In the anodic portion of the curve the formation of the corrosion products affects the development of the $E/\log i$ curve. When a metal M undergoes corrosion it is converted into ion in a process described by $M \rightarrow M^{z+} + ze^-$, where z represents that the metal atom can deliver more than one electron. An upward deviation of the $E/\log i$ curve is caused by decreased conductivity of anode. With time the corrosion products develop on the specimen surface and pass through various chemical reactions.

When Co corrodes in water over the broad range of pH concentration, several reactions directly influenced by the pH of a solution may take place:

(a) The usual anode reaction of Co dissolution



is only a short form for the chain of possible chemical reactions much better investigated in the case of iron corrosion, and probably comprises the following steps:



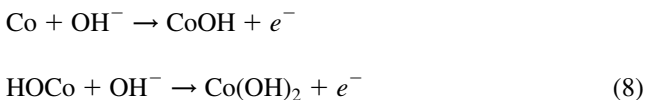
(b) The formation of cobalt hydroxide



(c) The dissolution of cobalt hydroxide by acid



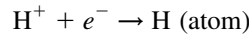
(d) The alkaline environment film formation reaction



The reactions in Eqs. (7) and (8) are directly influenced by the pH of electrolyte while the reactions in Eqs. (4), (6) and (8) that result in the generation of electrons are influenced by the variation of the electrode potential. The reaction kinetics in Eq. (8) can be influenced by both the pH of the solution and the applied electric potential.

The cathodic processes, taking place mostly in the elec-

trolyte at $\text{pH} < 7$ are



and involve the reduction of hydrogen ions to liberate hydrogen gas on the cathode, and at $\text{pH} \geq 7$



An imbalance of hydrogen and hydroxide ions in a solution has an influence on the value of the open circuit-corrosion potential and corrosion current, as can be concluded from Figs. 3 and 4. If the carbon overcoat is completely porous-free the value of the corrosion potential will be close to the value measured on the bulk carbon. For this analysis the reference carbon layer was formed as a pressed graphite powder and the value of E_{corr} was measured at pH 5.5. The lower found nobility of the hard disk carbon is mainly due to the film void structure, allowing water vapor permeation into the magnetic layer and chemical reactions on the surface with the constituents coming from the magnetic layer.

A comparable study was performed on another overcoat type, the amorphous tetrahedral carbon, ta-C, deposited by the filtered cathodic arc technique [20]. The film thickness was in the 5–15 nm range. With this deposition technique it is possible to produce compact film, with a density of up to 3.5 g/cm^3 , compared to sputter and ion beam deposited a-C:H:N films of average density around 2 g/cm^3 . In spite of the 100% coverage of the surface by only carbon atoms in this overcoat type, the porous structure of the overcoat led to shifting down of the value of the corrosion potential by more than 200 mV, with respect to the value of the bulk graphite. The corrosion potential of the bulk Co was found to be -0.69 V versus SCE in $0.1 \text{ N Na}_2\text{SO}_4$ solution [3]. Graphite and platinum, used as a counter electrode, are the noblest

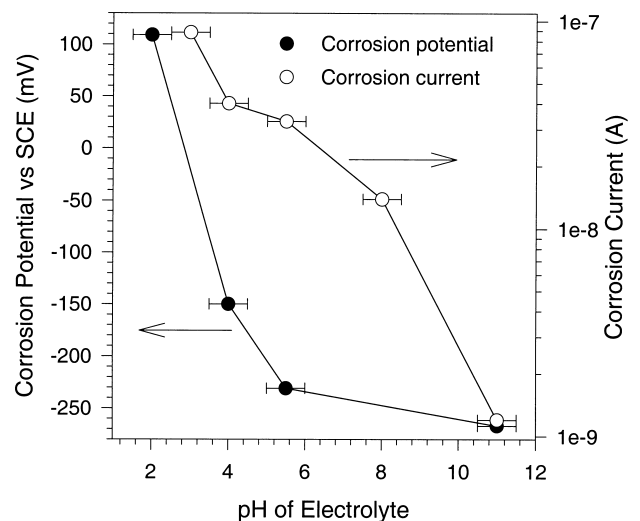


Fig. 4. Influence of pH of electrolyte on the corrosion current density and corrosion potential for the a-C:H:N overcoat.

materials with the highest free corrosion potential versus SCE in a solution similar to salt seawater.

A dependence of the corrosion current and voltage with pH of electrolyte for the nitrogenated a-C:H film is shown in Fig. 4. The values for the corrosion current were taken from the computer software procedure that generated the fitted curves on both the anodic and cathodic sides of the $E_{\text{corr}}/\log i$ curve. Also, some of the values were calculated from the anodic and cathodic Tafel slopes of the potentiodynamic curve and the $\Delta i/\Delta E$ slope of the DC polarization curve, implementing Eq. (1). A steady decrease of the corrosion current density with increasing pH of solution was observed. Similar behavior of the corrosion current density versus pH was found on another type of magnetic layer (with almost the same Co-content) without overcoat as well as with a tetrahedral a-C carbon overcoat on it. Dissolution of Co in an acid environment is larger than in alkaline. This has a direct implication on the expected lifetime of a hard disk operating in such an environment. The vulnerability of hard disk exposed to sulfur dioxide and chlorine gas has been related to the acid formation on the hard disk surface in the presence of humidity [10,13]. A decrease of the DLC film corrosion potential with increasing pH is influenced by the concentration of H^+ and OH^- ions in the electrolyte. The higher corrosion potential, at pH 2 and pH 4, is accompanied by a larger corrosion current. Independently from the higher dissolution rate of Co in acid, an increased potential drop between the carbon overcoat and magnetic layer opens the galvanic-induced corrosion channel. An exposure of the magnetic layer to humidity and aggressive environmental gases can be substantially reduced with carbon overcoat lubrication. Even one or two monolayers of lubricant can represent a good corrosion barrier. Corrosion also provokes evaporation and degradation of lubricant with Co emerging on the overcoat surface [21,22]. Due to the presence of Co in the lubricant a reduced number of the lubricant-to-carbon

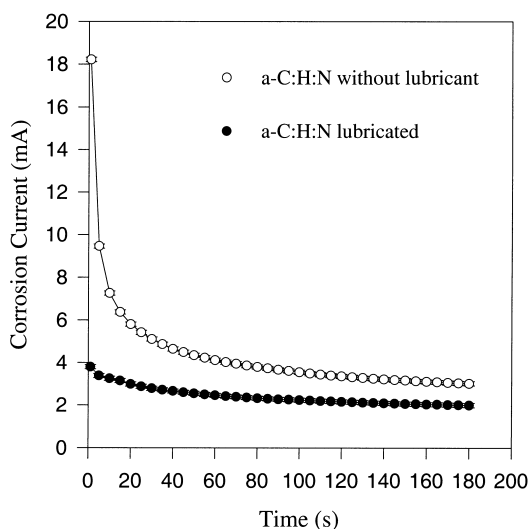


Fig. 5. Two-electrode cell electrochemical test of corrosion current on the lubricated and non-lubricated a-C:H:N overcoat.

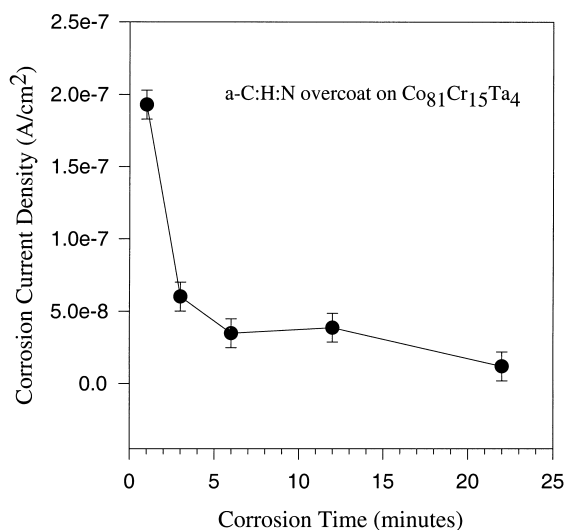


Fig. 6. Time development of the corrosion current after exposing the overcoat to the electrolyte at pH 5.5.

bond sites and increased friction between a slider and the overcoat are to be expected.

The corrosion current measured in a two-electrode cell for lubricated and non-lubricated nitrogenated a-C:H film is presented in Fig. 5. A constant voltage of 1.5 V is applied between the hard disk surface (anode) and graphite counter electrode. Between the two electrodes was placed a filter paper wetted in the electrolyte. The area under the i_{corr} versus time curve can serve as a measure for the corrosion current passing through the hard disk surface. This area is proportional to the charge flow. In order to exclude the portion of the curve when current saturation starts to develop the first 20 s of the current flow was selected as a convenient time interval. The same technique for the fast evaluation of the corrosion protective properties was reported in Ref. [10]. A total charge flow in that time interval Q_{20} for the lubricated and non-lubricated sample was 7×10^{-5} and 1.2×10^{-4} C, respectively. The lower value indicates better disk corrosion resistance.

The corrosion current measured by the DC polarization resistance technique and implementing Eq. (1) is presented in Fig. 6. Linear polarization curves were obtained in the voltage range ± 20 mV with respect to the open circuit potential. A scan speed of 0.166 mV/s was used starting from the cathodic side. Under the assumption that the anodic and cathodic Tafel slopes can be taken as constant, with measured values of 700 and 200 mV/decade, respectively, a series of DC polarization resistance curves was conducted with an average acquisition time of 2 min. Prior to acquisition samples were exposed to the electrolyte for varying purging times. An error made by taking the constant values of Tafel slopes for the specimens exposed to open circuit potential in the time interval between 3 and 22 min is relatively small. Saturation of the corrosion current with time may be explained by the formation of corrosion products under the filter paper and by the addi-

tional film resistance connected in series to the changeable electrolyte properties. The corrosion products in the form of cobalt hydroxide or chloride were trapped within the investigated sample area.

Several authors presented a depth profile analysis on the corrosion sites using Auger or X-ray photoelectron spectroscopy. Hard disks were exposed to the corrosive gases in an accelerated business environmental test [10,15], or to an electrolyte [14]. The preferential cobalt dissolution in the magnetic layer was stressed as well as Co migration to the overcoat surface and precipitation in the form of oxides and chlorides. The EC tests are more convenient for the fast evaluation of the corrosion properties of different magnetic materials, alone or in conjunction with the protective overcoat. The business environmental tests are more appropriate for lifetime and reliability evaluation of the hard disks exposed to different environmental gases and vapors. Migration of Co through the carbon overcoat is driven with the Co concentration gradient and carbon galvanic action. Under our testing conditions, that were very similar to those reported by Smallen et al. [10], the measured corrosion intensity Q_{20} was more than one order of magnitude lower than reported, giving rise to the conclusion of a smaller surface concentration of migrated Co and therefore of a better overcoat protection. Other supporting evidence is that the Co signal from the film surface was below the detection limit using the RBS technique in the geometry with the highest depth resolution, and by AES analysis in the acquisition area outside the corrosion hillock formation. Comparison of the corrosion current densities, that are in our case at least two orders of magnitude lower than in Ref. [11] (in NaOH/Na₂B₄O₇), or in Ref. [14] (in 0.1 N solution of Na₂SO₄), obtained in the three-electrode cell configurations may also indicate a better corrosion property of the investigated carbon overcoat.

The macroscopic magnetic properties of the corrosion treated samples were investigated from the film hysteresis loop, using a vibrating sample magnetometer. Within the experimental error no macroscopic changes in the magnetic properties were observed in the radial and axial direction, before and after a disk exposure to the EC test. A similar finding has been reported [14], and even a small increase in the film coercivity, ascribed to the effect of grain boundary corrosion, was observed [13]. Obviously, for this type of thin film corrosion study, a more appropriate technique would be the magnetic force microscopy of previously magnetically patterned hard disk.

An overcoat surface topography study has been performed with SEM and AFM. After the EC test, under the previously stated conditions, an average number of created corrosion sites in the form of hillocks was estimated to be around 1.2×10^6 defects/cm², as can be seen from Fig. 7. The size of defects varied around an average value of 1.5 μ m. The role of the carbon overcoat in preventing the lateral distribution of corrosion products, already stressed in Ref. [10], can be clearly seen from the AFM and SEM images. The corrosion products are not uniformly distributed across the overcoat. By detailed analysis over a larger surface area, corrosion products were found even with a lateral dimension of up to 12 μ m, as shown in Fig. 8. These products were created on places with large pinhole imperfections in the carbon overcoat. With AFM, pinholes were also detected on the uncovered magnetic film surface. This confirms the importance of the Cr undercoat deposition as a barrier for the Ni dissolution from the Ni₈₀P₂₀ layer, especially in the acid environment.

4. Conclusion

The potentiodynamic and polarization resistance method

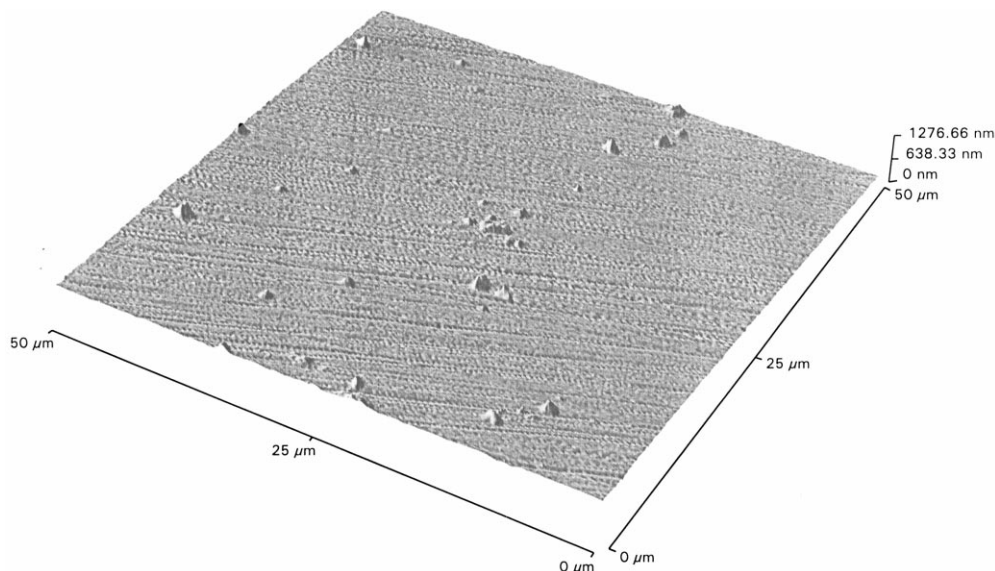


Fig. 7. Corrosion defects created on the DLC overcoat revealed by AFM analysis. The density of hillock formation is around 1.2×10^6 defects/cm².

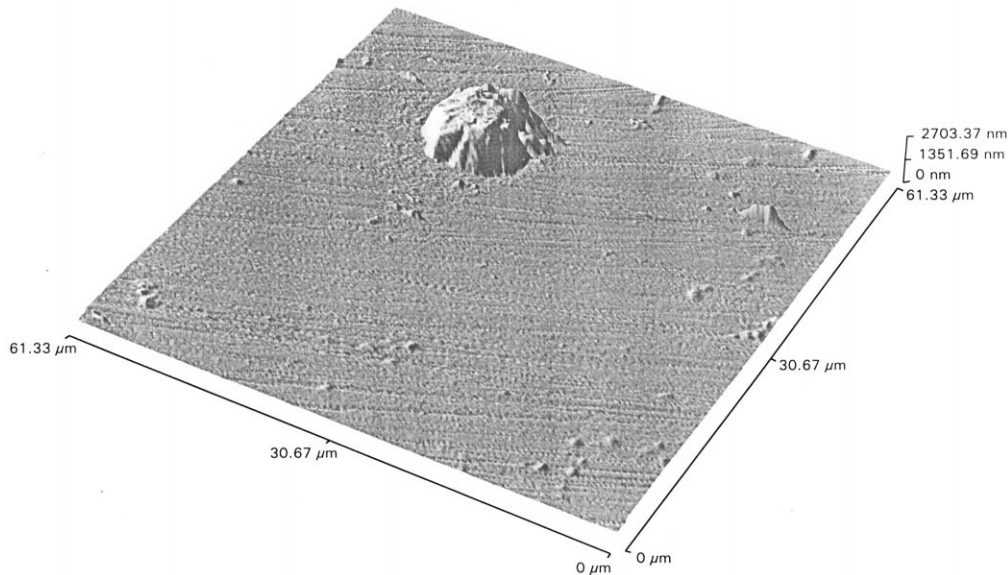


Fig. 8. The large pinhole in the carbon overcoat enabled the hillock build-up of corrosion products.

can be used for evaluation of the corrosion protective properties of different types of carbon overcoats as well as magnetic thin films. This type of test may give similar conclusions about the overcoat quality, in comparison to the accelerated business environment test that usually takes much more time to conduct. Implementation of EC tests is limited to the electrolyte environment and to the possible detrimental gases that can be dissolved in it. Though the accelerated business environmental tests are more realistic, EC tests can predict the behavior of different magnetic materials and protective overcoats at the stage of selection and design of the hard disk media.

More severe requirements on the quality of the carbon overcoat are imposed for the hard disk operation in the acid environment. This environment can also include the presence of different types of gases, like SO_2 and Cl_2 , that create acid on the hard disk surface in the presence of air humidity. The corrosion current density on the hard disk can be more than one order of magnitude higher by exposing a disk to an acid environment. Vulnerability of the magnetic layer to the dissolution in acid is closely related to the density of voids and pinholes in the carbon overcoat. The quality and effectiveness of the protective overcoat can be measured under specified conditions with the AFM and SEM technique, determining the surface density, size and shape of hillocks-corrosion sites. Even a very thin 1–2 nm lubricating layer deposited on the carbon overcoat can substantially decrease the corrosion current by preventing the permeation of the water vapor through the void structure of the overcoat. To minimize the galvanic action between the magnetic layer and the overcoat it is necessary to develop overcoats with high electrical resistance, in an ideal case with dielectric properties.

Acknowledgements

The authors would like to thank A. Chekanov for the help in the AFM analysis and M. Loh from the Physics Department, National University of Singapore, for providing us with Auger spectra of the depth distribution of Co atoms.

References

- [1] M.F. Doerner, R.L. White, *MRS Bull.* XX (10) (1996) 28.
- [2] H.-c. Tsai, D.B. Bogy, *J. Vac. Sci. Technol. A* 5 (1987) 3287.
- [3] J. Robertson, *Diam. Rel. Mater.* 3 (1994) 361.
- [4] J. Robertson, *Surf. Coat. Technol.* 50 (1992) 185.
- [5] S. Kumar, K.S.A. Butcher, T.L. Tansley, *J. Vac. Sci. Technol. A* 15 (1996) 2687.
- [6] M. Nakayama, Y. Matsuba, J. Shimamura, Y. Yamamoto, H. Chihara, H. Kato, *J. Vac. Sci. Technol. A* 14 (1996) 2418.
- [7] P. Zou, M. Scherge, D.N. Lambeth, *IEEE Trans. Magn.* 31 (6) (1995) 2985.
- [8] R. Prioli, S.I. Zanette, A.O. Caride, *J. Vac. Sci. Technol. A* 14 (1996) 2351.
- [9] J.S. Judge, J.R. Morrison, D.E. Spiliotis, *J. Electrochem. Soc.* 112 (1965) 681.
- [10] M. Smallen, P.B. Mee, A. Ahmad, W. Freitag, L. Nanis, *IEEE Trans. Magn.* 21 (5) (1985) 1530.
- [11] V. Brusica, M. Russak, R. Schad, G. Frankel, A. Selius, D. DiMilia, *J. Electrochem. Soc.* 136 (1) (1989) 42.
- [12] M. Yanagisawa, N. Shiota, H. Yamaguchi, Y. Sukanuma, *IEEE Trans. Magn.* 19 (1983) 1638.
- [13] R.R. Dubin, K.D. Winn, L.P. Davis, R.A. Cutler, *J. Appl. Phys.* 53 (1982) 2579.
- [14] V. Novotny, N. Staud, *J. Electrochem. Soc. Electrochem. Sci. Technol.* 135 (12) (1988) 2931.
- [15] V. Novotny, G. Itnyre, A. Homola, L. Franco, *IEEE Trans. Magn.* 23 (5) (1987) 3645.
- [16] D. Wang, W.D. Doyle, H.M. Saffarian, G.W. Warren, *IEEE Trans. Magn.* 31 (6) (1995) 2761.

- [17] Y. Yamamoto, K. Sumiya, A. Miyake, T. Taniguchi, *IEEE Trans. Magn.* 26 (5) (1990) 2098.
- [18] K. Tagami, *IEEE Trans. Magn.* 21 (5) (1985) 1435.
- [19] L.R. Doolittle, *Nucl. Instrum. Methods B9* (1985) 344.
- [20] F. Mansfield, in: M.G. Fontana, R.W. Staehle (Eds.), *Advances in Corrosion Science and Technology*, 6, Plenum Press, New York, 1976, p. 163.
- [21] S. Xu, B.K. Tay, H.S. Tan, et al., *J. Appl. Phys.* 79 (9) (1996) 7234.
- [22] L.J. Huang, Y. Hung, S. Chang, *IEEE Trans. Magn.* 33 (6) (1997) 4551.